11 SCIENTIFIC HIGHLIGHT OF THE MONTH

Electric transport perpendicular to the planes

Heike C. Herper

Gerhard-Mercator Universität, Institute of Physics, D-47048 Duisburg, Germany
and
Center for Computational Materials Science TU-Vienna, A-1060 Vienna, Austria

Abstract

Since the discovery of the giant magnetoresistance (GMR) in magnetic multilayers several theoretical descriptions have been used to determine the resistivity of such a layered structure. Though the resistance for the current in direction of the planes of layers can easily be measured and has been intensively studied in theoretical works [1, 2], the GMR for the current perpendicular geometry (CPP) is slightly more difficult to describe. Here, a formalism for the investigation of the CPP GMR is reported by making use of the Kubo-Greenwood equation. This formalism is a useful tool for the discussion of the influence of the interfaces on the GMR. The presentation of the Kubo-Greenwood formalism for CPP transport is complemented by a brief discussion of some results.

1 Introduction

The behavior of two magnetic layers separated by a nonmagnetic material strongly depends on the magnetic configuration of the two magnets. Usually the resistance of the system drops down if a magnetic field is applied and, therefore, the magnetic moments of the two magnets are parallel aligned. This effect is known as giant magnetoresistance (GMR) and has been intensively studied during the last fifteen years [3, 4]. The above described GMR is somehow different from the *natural* magnetoresistance effect (anisotropic magnetoresistance = AMR, Hall effect). The AMR, can be observed in every metal due to the Lorentz force on the conduction electrons and depends on the angle between the magnetization and the current [5, 6]. This magnetoresistance

is caused by the fact that the magnetization in thin films is not homogenous, but is influenced by domain walls and other impurities, which means the resistance measured parallel to the magnetization direction is different from the resistance perpendicular to the magnetization direction of the film. It has been tried to use the AMR for technical purposes, but the applications were restricted to low temperatures.

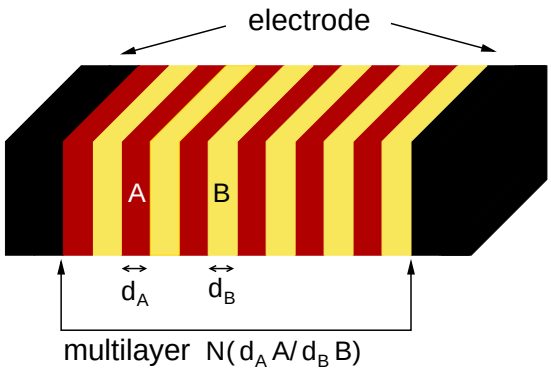

Figure 1: Schematic drawing of a multilayered structure, which consists of alternating layers of material A and B. The thickness of the layers is denoted by d_A and d_B. The multilayer is covered by two magnetic leads (electrodes).

The situation started to change, when Baibich and others observed the GMR effect in sandwich structures, Fe/Cr/Fe in particular. Similar trilayered structures have been already used to examine the tunneling magnetoresistance in FM/SC/FM (SC = semiconductor) sandwiches so called tunnel junctions [7, 8]. The GMR has the advantage that it is usually larger than the AMR and is suitable for measurements at elevated temperatures [9]. In contrast to the AMR the GMR occurs only in systems in which an external magnetic field can change the magnetic configuration of the system or in other words the coupling between the layers is not too strong or even FM. However, for practical purposes the GMR of a single FM/NM/FM trilayer (FM = ferromagnetic, NM = nonmagnetic) is still too small, but it has been observed that the effect can be increased by using more complex multilayer structures (Fig. 1).

The fact that the magnetic configuration in such materials can easily be switched by a magnetic field makes them interesting for technological applications. Several fabrication techniques have been developed in the past, which allow to built high quality superlattices, multilayers or spin-valves [4]. These systems can generally divided in two classes: coupled and non-coupled systems. In coupled structures the magnetic configuration of both magnets is influenced by the external field, whereas in non-coupled (e.g. spin-valve) systems the magnetic configuration of one FM is kept fixed by an additional anti-ferromagnetic (AF) layer [10]. Today, the GMR is already used in reading heads of CD disc drives and for magnetic data storing – MRAM technology [11, 12]. It should be mentioned that for technical purposes often systems with semi-conducting spacers are used, which means making use of the TMR effect.

As mentioned above the GMR is caused by a magnetic field, which changes the scattering of the conduction electrons [6]. However, the electric transport properties of multilayers are also influenced by the preparation technique, temperature etc. [13]. These effects determine the

structure of the interface, e.g. the occurrence of interdiffusion and alloy formation. Furthermore, the GMR depends on the thickness of the NM and FM layers. Closely related to these topics is the question of the interlayer exchange coupling (IEC) in such systems, because it has been shown that AF coupling supports the possibility of spin-dependent transport and gives possibilities for practical applications [14].

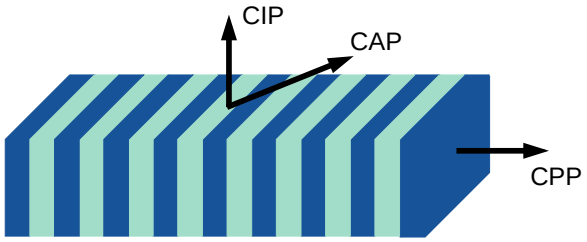

Figure 2: Different geometries are possible for GMR studies. Mainly two configurations are used: current perpendicular to the planes (CPP) and current in plane (CIP) geometry. In general the current has a certain angle to the planes (CAP).

Besides the above mentioned features, the size of the GMR in a layered structure also depends on the experimental setup. The easiest way to measure a resistance in a multilayer is for current in plane (CIP) geometry, see Fig. 2. The CIP GMR can be quite large. Unfortunately, the CIP resistance is not very interesting for technical applications, because the important features of a multilayer occur in growth direction. In addition, measurements in CIP geometry are not sufficient to determine the current density [15]. In contrast to that measurements with the current perpendicular to the planes (CPP) give very accurate results. Though, measurements in CPP geometry are much more complicated as compared to CIP experiments [4, 16] the CPP GMR may be important for applicational purposes at low temperatures ($\leq T_{\mathrm{room}}$), because it is large as compared to the CIP MR [16, 17].

Today, several preparation techniques exist making use of the CPP GMR and related phenomena in magnetic multilayers, see Ref. [16, 18]. Nonetheless, there is still no real consense what the main cause of the GMR is: the connection between the electronic band-structure and the magnetic moments of the layers or the spin-dependence of the single-site scattering potentials [19]. Besides that there exists a number of more practical questions, which depend on the particular system, e.g. how does interdiffusion influences the size of the GMR and how are the GMR and IEC related? The calculational approaches used to investigate the resistances range from the semi-classical Boltzmann theory [5] to quantum-mechanical descriptions, e.g. the Kubo-Greenwood equation [19, 20, 21]. A third method intensively used for the examination of ballistic transport in tunnel-junctions is the Landauer-Büttiker method. This method describes transport properties on a mesoscopic scale, which means that the results depend on the size of the sample. The resistances are measured far away from the FM/NM interfaces. Therefore, a description of effects near the interfaces is somewhat difficult to include. However, the structure of the interface can be described quite easily within the Kubo-Greenwood approach. Alloy formation, impurities and other effects can be included in the calculation. This may be important for the comparison with the measurements and the interpretation of the experimental findings.

A detailed description of the Kubo-Greenwood equation and its application to layered structures is presented in Sec. 3. Before that, in Sec. 2 an overview of relevant experimental results and technique is given. Finally, some results concerning CPP transport in Fe/Cr/Fe and Fe/Si/Fe sandwiches will be discussed in Sec. 4.

2 CPP transport from the experimental point of view

In this section some fundamental experimental results concerning GMR effect and related properties are presented. Results for the TMR are not shown. The GMR effect can be measured between a FM and any disordered magnetic state of the multilayer. Usually the GMR ratio is defined as the change of the resistance under a magnetic field **H** (FM solution) relative to the resistance of the zero field state R^0

$$R^{\exp} = \frac{R^0 - R^H}{R^0}. \tag{1}$$

Today, some authors use the saturation state instead of the zero field state, because in this case the contribution from spin disorder is minimized [6]. In theoretical calculations it is convenient to assume that the zero field state corresponds to a perfect AF arrangement of the magnetic moments of the leads, where effects of spin disorder etc. are neglected. The GMR is then given by the difference between the parallel (FM) and antiparallel (AF) solution, whereby R^0 is replaced by R^{FM}

$$R = \frac{R^{\mathrm{FM}} - R^{\mathrm{AF}}}{R^{\mathrm{AF}}}, \quad R \leq 1. \tag{2}$$

Here, the difference of the resistances is divided by the anti-ferromagnetic configuration R^{AF}, which gives a bounded solution provided that $R^{\mathrm{AF}} > R^{\mathrm{FM}}$. It is also common to use an unbounded solution dividing by R^{FM} instead of R^{AF}.

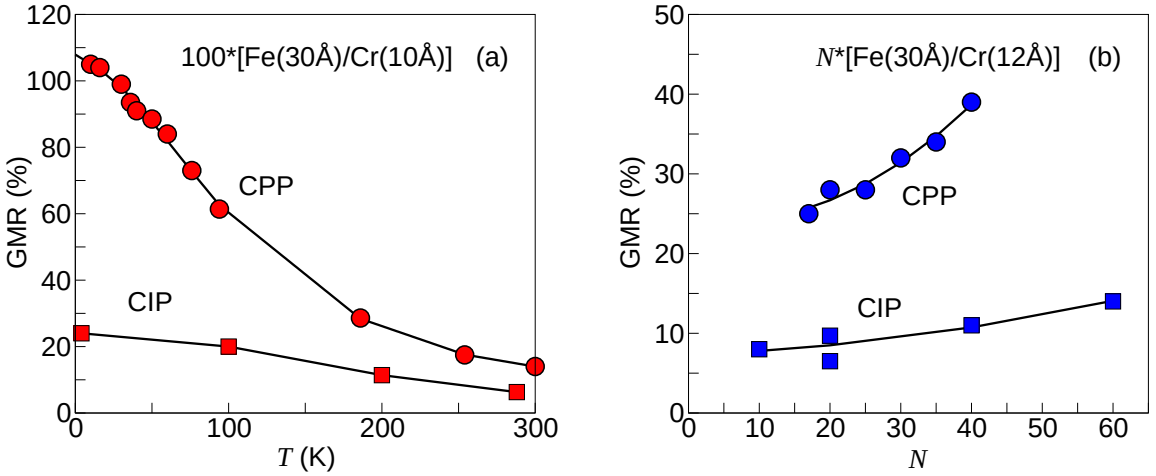

Figure 3: Measured GMR of Fe/Cr multilayers at varying temperatures (a) and depending on the number of bilayers N (b). The experimental data are taken from the Refs. [16] and [22].

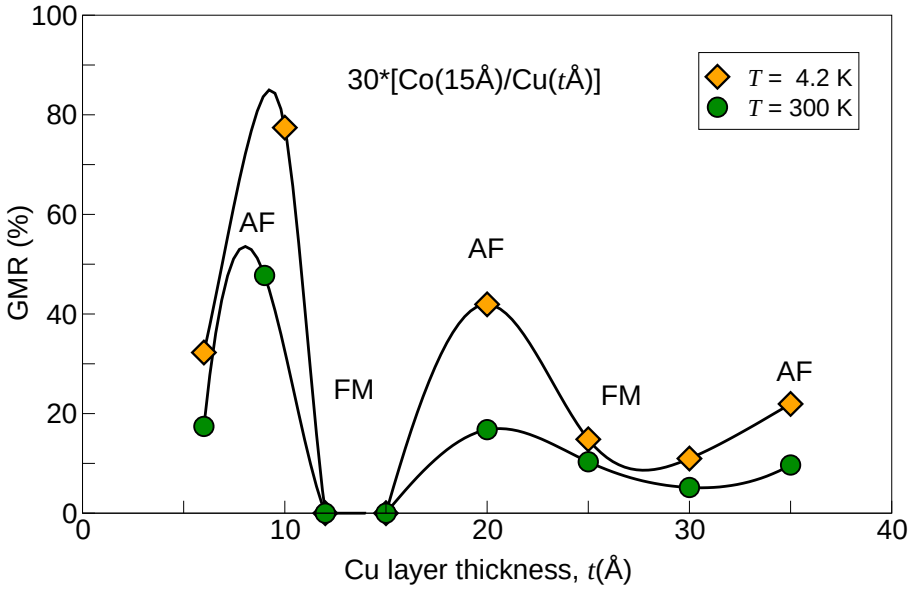

Figure 4: Measured GMR of Co/Cu multilayers with varying thickness of the Cu layers t. The oscillations can be related to the oscillations of the interlayer exchange coupling of the Co layers. The data are taken from Ref. [23].

Some typical experimental results for the GMR of the most famous multilayers: Fe/Cr and Co/Cu, are reproduced in the Figs. 3 and 4. It is known that the size of the GMR depends on the temperature (Fig. 3a). At low temperatures the CPP GMR is much larger as compared to the GMR measured in CIP geometry, which was predicted before by several theoretical investigations [24, 25]. With increasing temperature the difference between CIP and CPP GMR becomes smaller and in some cases the CIP GMR may become larger than the CPP one [16]. In addition, the GMR of a multilayered structure depends on the number of bilayers, e.g. repetition of the two components (Fig. 3b). In the case of Fe/Cr it has been observed that the size of the CPP GMR strongly increases with growing number of repetitions N, whereas the CIP GMR is not much effected by N (Fig. 3b). Furthermore, the GMR of a Co/Cu multilayer is shown in Fig. 4 depending on the thickness of the NM Cu layer. The size of the GMR strongly oscillates with the thickness of the Cu layer. It has been shown that these oscillations are related to the interlayer exchange coupling of the two leads [3].

3 Electric transport within the Kubo-Greenwood formalism

3.1 Kubo-Greenwood equation

In order to determine the resistance of a layered system described in the previous section we can make use of Kubo's method [20]. The Kubo formula describes the response of a quantum mechanical system to an external field, e.g. the change of the electric current due to an electric field, whereby it is assumed that the perturbation is small and therefore the relation between

field and current can be assumed to be linear. In this case the Hamiltonian of the original system is modified by a perturbation $\widehat{\mathbf{H}}'$

$$\widehat{\mathbf{H}} = \widehat{\mathbf{H}}_\mathbf{0} + \widehat{\mathbf{H}}', \tag{3}$$

where $\widehat{\mathbf{H}}_\mathbf{0}$ describes the unperturbated system. Here, the perturbation is chosen to be

$$\widehat{\mathbf{H}}' = -\mathbf{pE} \tag{4}$$

assuming that the electric field $\mathbf{E}$ is a periodic quantity and $\mathbf{p}$ the electric dipole-moment

$$\mathbf{E} = \mathcal{E} e^{-i(\omega+i\delta)t}. \tag{5}$$

The present choice of $\mathbf{E}$ ensures that the perturbation vanishes for $t = -\infty$ if $\delta \to 0$. In linear response the electric current is related to the electric field by the two-point conductivity tensor $\underline{\underline{\sigma}}(\mathbf{r}, \mathbf{r}')$

$$\mathbf{j}(\mathbf{r}) = \int d^3r' \underline{\underline{\sigma}}(\mathbf{r}, \mathbf{r}')\mathbf{E}(\mathbf{r}'). \tag{6}$$

In the limit of static, homogeneous electric fields, i.e. in the zero frequency limit, the Kubo approach yields for the conductivity [20, 26, 27]

$$\underline{\underline{\sigma}}(\mathbf{r}, \mathbf{r}') = -\lim_{\omega\to 0} \frac{1}{\omega} \underline{\underline{\Pi}}(\mathbf{r}, \mathbf{r}', \omega) \tag{7}$$

with $\Pi(\mathbf{r}, \mathbf{r}', \omega)$ being the current-current correlation function

$$\underline{\underline{\Pi}}(\mathbf{r}, \mathbf{r}', \omega) = \frac{1}{V} \int_0^\infty d\tau e^{i\omega\tau} \langle \left[\widehat{\mathbf{j}}(\mathbf{r}, t+\tau), \widehat{\mathbf{j}}(\mathbf{r}', t)\right] \rangle, \tag{8}$$

in which V denotes the unit volume. Here, $\langle \quad \rangle$ denotes the expectation value over all states of the system at zero temperatures and $\widehat{\mathbf{j}}(\mathbf{r}, t)$ is the quantum mechanical current operator

$$\widehat{\mathbf{j}}(\mathbf{r}, t) = e^{i\widehat{H}_0 t} \widehat{\mathbf{j}}(\mathbf{r}) e^{-i\widehat{H}_0 t}, \qquad \widehat{\mathbf{j}}(\mathbf{r}) = \frac{e\hbar}{mi} \psi^\dagger(\mathbf{r}) \underline{\nabla_r} \psi(\mathbf{r}). \tag{9}$$

Finally, Eq. (8) leads to the Kubo-Greenwood equation for the electric conductivity

$$\sigma_{\mu\nu} = \frac{\pi\hbar}{V} \langle \sum_{mn} j^\mu_{mn} j^\nu_{nm} \delta(\epsilon_\mathrm{F} - \epsilon_m) \delta(\epsilon_\mathrm{F} - \epsilon_n) \rangle, \tag{10}$$

with μ and ν denoting the Cartesian indices x, y, z [20, 26]. The expression in Eq. (9) holds only for nonmagnetic metals. However, at least the lead material of a multilayer is magnetic, which leads to charge and spin accumulation effects. This problem can be overcome by introducing spin-dependent current densities, see for example Refs. [21, 28].

3.2 Application to layered structures

The general expressions discussed in Sec. 3.1 can be simplified assuming a layered structure which provides two-dimensional translational symmetry. Suppose the layers grow along the z-axis and the fields in the $(x-y)$-plane are homogeneous then Eq. (6) reduces to

$$\mathbf{j}(z) = \int dz' \underline{\underline{\sigma}}(z, z')\mathbf{E}(z') \tag{11}$$

Usually transport measurements are carried out for current in the $(x-y)$-plane (CIP) or perpendicular to the plane (CPP) geometry, compare Fig. 2. For fields in the CIP case the calculation of the $\underline{\underline{\sigma}}(z,z')$ matrix is straight forward, because the electric field in z-direction is constant. This leads to

$$j(z) \;=\; E \int dz' \underline{\underline{\sigma_{\parallel}}}(z,z'). \tag{12}$$

Until now the current is still a microscopic quantity. The measured current corresponds to the expectation value of the current divided by the system size, i.e. length of the system in growth direction L

$$\langle j(z) \rangle \;=\; E \frac{1}{L} \int dz dz' \sigma_{\parallel}(z,z') \;=\; E\,\sigma_{\mathrm{CIP}}. \tag{13}$$

The situation becomes more complex if we apply the electric field perpendicular to the planes. In this case the electric field $E(z)$ is no longer constant. However, it will be shown that the transport in CPP geometry can be handled similarly to the CIP case assuming steady state conditions [6]. In order to discuss perpendicular transport it is more convenient to use the inverse of Eq. (11)

$$E(z) \;=\; \int dz' \rho_{\perp}(z,z') j(z'). \tag{14}$$

In the steady state the electronic density is time-independent, i.e. $\partial\rho/\partial t = 0$. Due to the continuity equation

$$\frac{\partial \rho}{\partial t} + \nabla \mathbf{j} = \frac{\partial \rho}{\partial t} + \frac{\partial j}{\partial z} \;=\; 0 \tag{15}$$

it follows that Eq. (15) is fulfilled only if the current is constant. In this case Eq. (14) can be rewritten

$$E(z) \;=\; j \int dz' \rho_{\perp}(z,z'). \tag{16}$$

The microscopic quantities in Eq. (16) can now be used to express the measured electric field, which is at least the average divided by the system size L

$$\langle E \rangle \;=\; j \frac{1}{L} \int dz dz' \rho_{\perp}(z,z') \;=\; j\,\rho_{\mathrm{CPP}}, \tag{17}$$

where ρ_{CPP} corresponds the measured resistivity.

The last step is to determine the resistivity or sheet resistance (see next section) of a layered system. However, from the Kubo-Greenwood formula Eq. (10) the conductivity is known, therefore one has to solve the following integral equation to obtain the resistivity ρ_{CPP} Eq. (17) of the system

$$\int dz'' \sigma_{\perp}(z,z'') \rho_{\perp}(z'',z') \;=\; \delta(z-z'), \tag{18}$$

which means inverting the conductivity matrix

$$\rho_{\perp}(z,z') \;=\; \sigma_{\perp}^{-1}(z,z'). \tag{19}$$

3.3 Sheet resistance

In our calculations we use the so called sheet resistance being the product of the resistivity and the system length

$$r = L\rho_{\mathrm{CPP}} = \int dz dz' \rho_{\perp}(z, z'), \tag{20}$$

where z and z' are still continuous variables perpendicular to the planes. The purpose of the following transformation is to map the conductivity tensor $\sigma(z, z')$ on a discrete expression for layered systems σ_{pq}^{zz}, with p and q denoting planes of atoms

$$\sigma(z, z') \longrightarrow \sigma_{pq}^{zz'}(n), \tag{21}$$

whereby n is the total number of layers taken into account. Due to the symmetry of the problem the mapping concerns only the z-components and the index z is suppressed in the following discussion. The mapping should conserve the formal structure of the problem such that yields

$$\int dz'' \sigma(z, z'')\rho(z'', z') = \delta(z - z') \longrightarrow \sum \sigma_{pr}(n)\rho_{rq}(n) = \delta_{pq}. \tag{22}$$

The necessary condition for the transformation in Eq. (22) is that the Cauchy convergence criterion is fulfilled. Here, the Cauchy criterion corresponds to

$$\left| r - \lim_{n\to\infty} r(n) \right| < \epsilon, \quad n \in N^{+}, \tag{23}$$

with ϵ being an infinitesimal small number. In this case the integral in Eq. (20) can be replaced by the sum over the planes of atoms

$$r(n) = \sum_{p,q=1}^{n} \rho_{pq}(n). \tag{24}$$

If the above mentioned conditions are fulfilled Eq. (24) can be used to calculate the sheet resistance of a layered system in CPP geometry. However, it should be kept in mind that the actual quantity, which is interesting in electric transport, is the change of the resistance due to an applied magnetic field, see Sec. 1. Therefore, it has to be taken into account that the sheet resistance also depends on the magnetic configuration of the leads $\mathcal{C}$. The two configurations considered in the calculations are displayed in Fig. 3. Therein, the leads used to be semi-infinite systems, i.e. bulk potentials or vacuum, which cover the spacer layers [19].

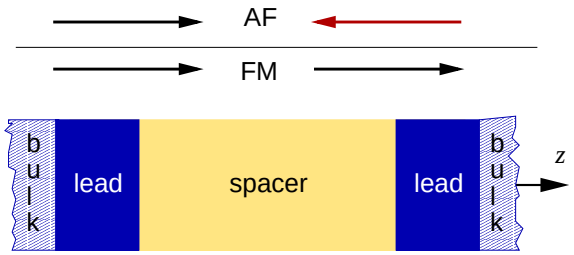

Figure 5: Schematic drawing of a trilayer. The NM spacer is covered by two semi-infinite FM leads (bulk), whereby some additional lead layers are used as buffer layers in the selfconsistent calculation (dark part). The two magnetic configurations used for the calculation of the GMR are marked by the arrows.

The FM configuration agrees with the experimental solution for an applied magnetic field and the AF case corresponds to the zero field situation, see Sec. 2. Due to technical reasons, i.e.

k-space integration and the handling of the surface Green's function it is helpful to evaluate the Kubo-Greenwood equation for a small but finite imaginary part of the Fermi energy $\epsilon_F - i\delta$. The actual sheet resistance for $\delta \to 0$ is then determined by

$$r(\mathcal{C}, n) \;=\; \lim_{\delta \to 0} r(\mathcal{C}, n, \delta) \;=\; \lim_{\delta \to 0} \sum_{p,q=1}^{n} \rho_{pq}(\mathcal{C}, n, \delta). \tag{25}$$

Accordingly, using the definition in Eq. (2) the CPP magnetoresistance within the Kubo-Greenwood formalism is given by

$$R(n) \;=\; \frac{r(\mathrm{AF}, n) - r(\mathrm{FM}, n)}{r(\mathrm{AF}, n)}. \tag{26}$$

In addition to Eq. (25) a layer-resolved sheet resistance can be defined by

$$r_p(\mathcal{C}, n) \;=\; \sum_{q=1}^{n} \rho_q(\mathcal{C}, n). \tag{27}$$

This expression can be used for a detailed discussion of the origin of the resistance, see Sec. 4.

Two problems arise from the above definition Eq. (26). First, charge and spin accumulation effects, which occur at the lead-spacer interface, require that a particular number of lead layers is included in the selfconsistently calculated part of the multilayer (dark regions in Fig. 5). It can be shown that for a sufficient large number of lead layers and a given value of δ the sheet resistance varies linear with n. For $\delta \to 0$ the sheet resistance is then independent from the number of lead layers, for details see Ref. [29]. A typical example is displayed in Fig. 6a for a $Fe_{12}/Si_9/Fe_{12}$ trilayer and $\delta = 2\,\mathrm{mRy}$.

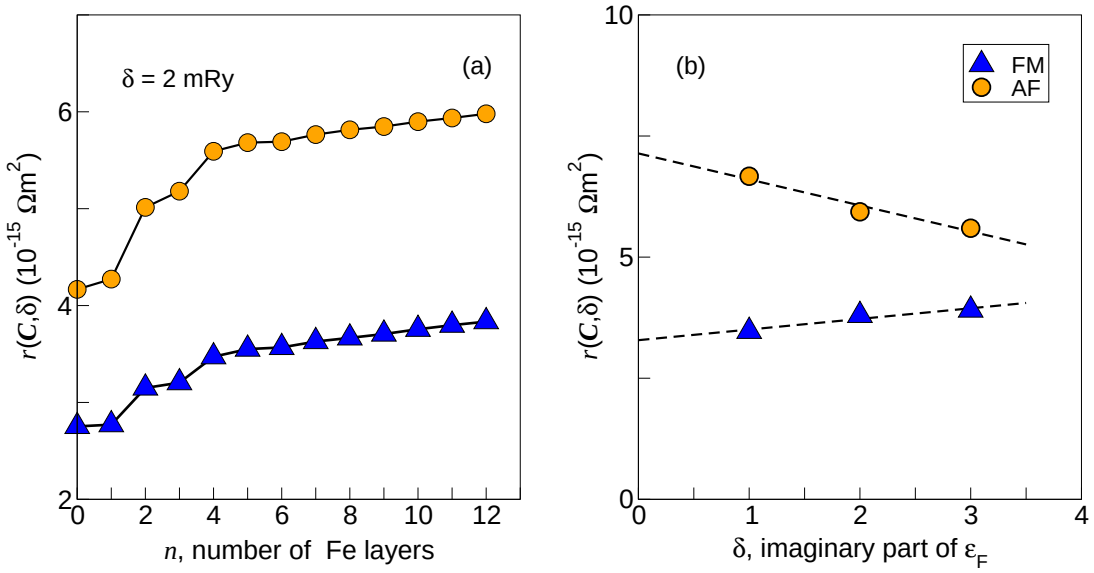

Figure 6: Variation of the sheet resistance $r(C, n, \delta)$ with the number of Fe lead layers n (a) and with the imaginary part of the Fermi energy δ (b) for a $Fe_{12}Si_{12}Fe_{12}$ trilayer. In both cases the results are shown for the AF (triangles) and FM (circles) alignment of the leads.

Second, from Eq. (25) it is obvious that the sheet resistance depends on the imaginary part of the Fermi energy. However, the sheet resistance varies linearly with δ provided the number of buffer (lead) layers is large enough, see Fig. 6b. Therefore, the actual sheet resistance can be obtained from calculations for finite δ [29].

4 Some results

In this section some numerical applications of the approach for CPP transport in layered structures (see Sec. 3.2) will be presented. All numerical input, which is necessary for the calculation of the sheet resistance Eq. (24), has been obtained from the fully-relativistic spin-polarized version of the screened Korringa-Kohn-Rostoker (SKKR) method [30, 31]. Technical details concerning the calculation of the electronic and magnetic properties can be found in Refs. [29, 32].

Basically the GMR is calculated for different spacer thicknesses, i.e. different numbers of NM layers, compare Fig. 5. A typical result of the GMR is displayed in Fig. 7a for a Fe/Cr/Fe trilayer. The GMR is plotted versus the number of Cr layers, whereby the Cr thickness ranges from 2 ML to 42 ML. With increasing number of Cr layers the GMR decreases from 28 % to $\approx 5\,\%$. However, the decrease is accompanied by oscillations, which depend on the number of Cr layers. In order to show that the oscillations are related to the interlayer exchange coupling (IEC) the energy difference between the two magnetic

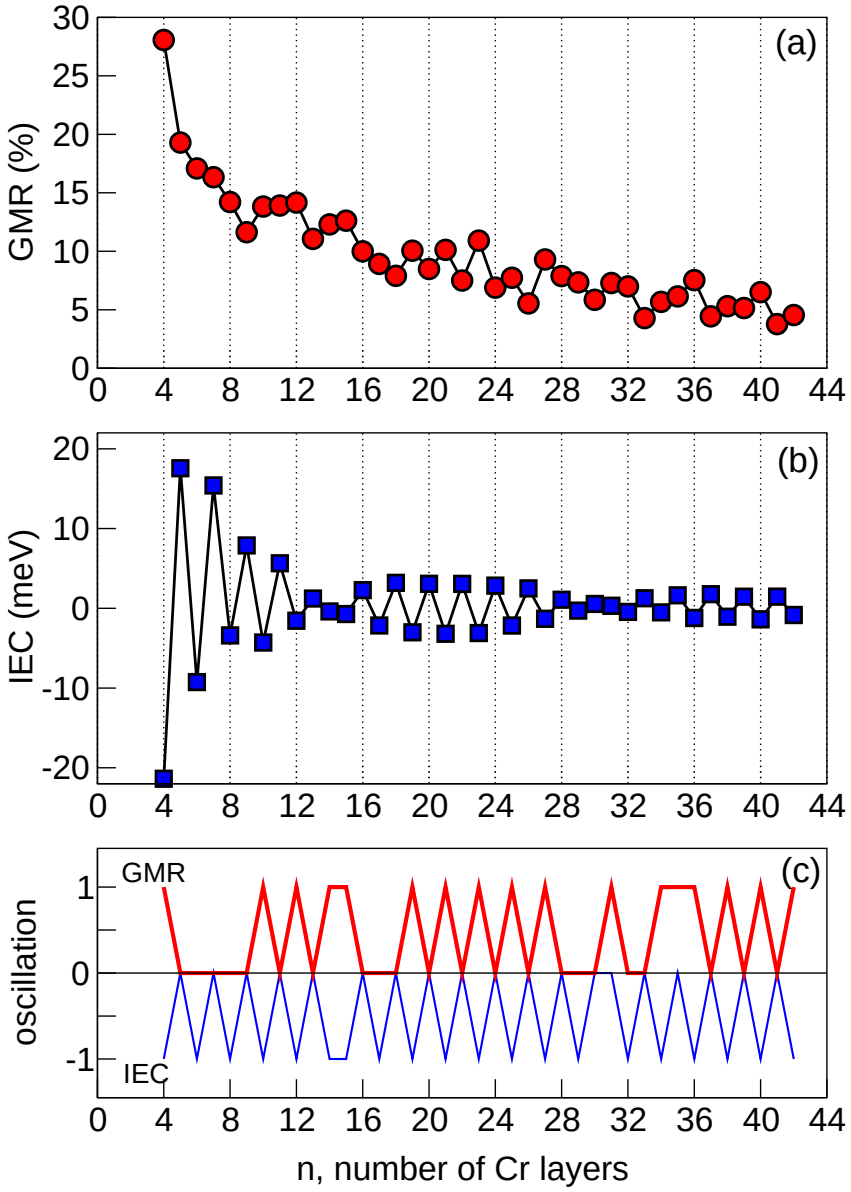

Figure 7: (a) The GMR of Fe/Cr/Fe trilayers depending on the number of Cr layers n. (b) Interlayer exchange coupling (IEC) for Fe/Cr/Fe obtained from the band energy difference vs. the number of spacer layers n. (c) Comparison of the oscillations of the GMR and the IEC of the above shown trilayers, for details see text. Data are taken from Ref. [33].

states $\Delta E = E(\mathrm{AF}) - E(\mathrm{FM})$ has to be examined. In here, the IEC has been obtained by applying the magnetic force theorem [30, 32]. The results are given in Fig. 7b. The oscillations of the GMR and IEC have been compared by checking whether the GMR(n) < GMR(n+1) or vice versa. In the first case the value of the oscillation for the (n+1)-layer system is set to one, whereas in the second case it is chosen to be zero. A similar procedure has been used for the IEC choosing zero for AF coupling and -1 for FM coupling, respectively. The results are summarized in Fig. 7c. From this viewgraph it is obvious that the two ML period of the IEC can be observed in the GMR. In addition, the phase slips occurring every 15-16 ML also exist,

but they are slightly shifted and smeared out. In this system the local minima in the GMR correspond to FM coupling and the maxima to AF coupling, respectively.

Furthermore, this method can also be used to examine systems with some configurational disorder, which may occur at the interfaces by interdiffusion. The disorder is described within the coherent potential approximation (CPA). That the CPA concept is sufficient for layered systems was shown in a previous paper [19]. An example for a system in which interdiffusion effects are important is Fe/Si. This system tends to build CsCl-like FeSi alloys near the interfaces [34]. In our calculations we have assumed that the interdiffusion region is restricted to the direct interface [32]

$$\ldots \mathrm{Fe/Fe}_{1-c_\mathrm{d}}\mathrm{Si}_{c_\mathrm{d}}/\mathrm{Fe}_{c_\mathrm{d}}\mathrm{Si}_{1-c_\mathrm{d}}/\mathrm{Si}_{s-2}/\mathrm{Fe}_{c_\mathrm{d}}\mathrm{Si}_{1-c_\mathrm{d}}/\mathrm{Fe}_{1-c_\mathrm{d}}\mathrm{Si}_{c_\mathrm{d}}/\mathrm{Fe}\ldots$$

The GMR obtained from Eq. (2) for different interdiffusion concentrations c_d is shown in Fig. 8. The calculations have been performed for three particular systems with 6, 9, and 12 ML of Si taking into account a two-layer interdiffusion. For $c_\mathrm{d} = 0$ the GMR is extremely large (50 %), which has not been reported in any experiment. However, independently from the number of spacer layers the GMR immediately breaks down if alloy formation takes place at the interfaces (Fig. 8).

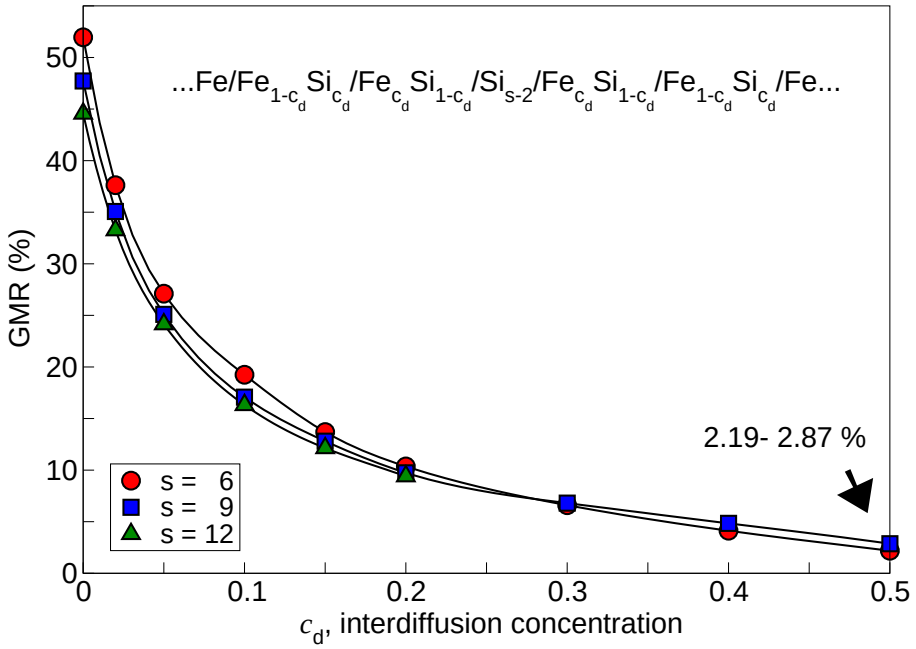

Fig. 8: GMR for Fe/Si$_s$/Fe trilayers vs. the interdiffusion concentration c_d for different spacer thicknesses s. Data are taken from Ref. [32]

If the interdiffusion reaches 20 % the GMR is already reduced to a fifth of the value for $c_\mathrm{d} = 0$. It is known from the literature that a $\mathrm{Si}_{0.5}\mathrm{Fe}_{0.5}$ alloy is quite likely to occur at the Fe/Si interfaces [34, 35]. The GMR of Fe/Si systems lie below 2.2 % [36, 37]. The present calculation for $c_\mathrm{d} = 0.5$ (Fig. 8) are in a good agreement with the experimental findings, which allow the conclusion that the small GMR of Fe/Si multi- or trilayers is strongly related to the formation

of Fe/Si alloys at the interfaces.

The GMR obtained from Eq. (2) and Eq. (24) provides only information for the whole trilayer. In order to check which layers or parts contribute mostly to the GMR it is helpful to use sheet resistance fractions. These fractions can be obtained from Eq. (27) by investigating the differences of the layer-resolved sheet resistances for the leads (region I and V), the spacer (III), and the interfaces (II and IV). An example is shown in Fig. 9 for the $Fe_{12}/Si_6/Fe_{12}$ system. From this figure it is obvious that the main contribution stems from the interfaces. In the case of $c_d = 0$ there still exists a reasonable large contribution (20 %) from the spacer. With increasing interdiffusion the latter one becomes smaller and vanishes at least for $c_{\mathrm{d}} = 0.2$. The contributions from the leads are negligible.

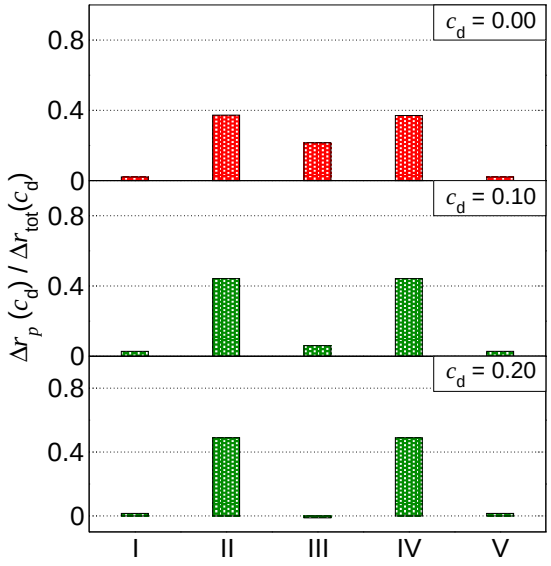

Figure 9: Normalized fractions of the layer-resolved sheet resistance differences Δr_p for characteristic regions p of $Fe_{12}/Si_6/Fe_{12}$. In the upper panel the results for the system with ideal interfaces are shown. The results for interface alloying are displayed in the middle and bottom panel. Roman numbers mark particular regions of the system: I left lead, II left interface, III spacer, IV right interface, and V right lead.

Acknowledgment

This work has been partially funded by the RT-Network *Computational Magnetoelectronics* and German Science Foundation through the Sonderforschungsbereich 491 *Magnetic Heterostructures: Structure and Electronic Transport.*

References

[1] C. Blaas, P. Weinberger, L. Szunyogh, P. M. Levy, and C. B. Sommers, Phys. Rev. B **60**, 492 (1999).

[2] W. H. Butler, Phys. Rev. B **31**, 3260 (1985).

[3] A. Fert, P. Grünberg, A. Berthélémy, F. Petroff, and W. Zinn, J. Magn. Magn. Mater. **140-144**, 1 (1995).

[4] *Spin dependent transport in magnetic nanostructures*, edited by S. Maekawa and T. Shinjo (Taylor & Francis, London, 2002).

[5] N. W. Ashcroft and N. D. Mermin, *Solid State Physics* (Harcourt, USA, 1976).

[6] P. M. Levy, *Solid state physics* (Academic Press, Cambridge, 1994), Vol. 47.

[7] M. Julliere, Phys. Lett. **54**, 225 (1975).

[8] N. Tezuka and T. Miyazaki, J. Appl. Phys. **79**, 6262 (1996).

[9] M. N. Baibich, J. M. Broto, A. Fert, F. N. V. Dau, and F. Petroff, Phys. Rev. Lett. **61**, 2472 (1988).

[10] B. Dieny, V. S. Speriosu, S. S. P. Parkin, B. A. Gurney, D. R. Wilhoit, and D. Mauri, Phys. Rev. B **43**, 1297 (1991).

[11] R. E. Matick, *Computer storage systems and technology* (Wiley & Sons, New York, 1976).

[12] S. S. P. Parkin *et al.*, J. Appl. Phys. **85**, 5828 (1999).

[13] J. Bass and W. P. P. Jr., J. Magn. Magn. Mater. **200**, 274 (1999).

[14] A. Muñoz-Martin, C. Prieto, C. Ocal, J. L. Martínez, and J. Colino, Surf. Sci. **482-485**, 1095 (2001).

[15] M. A. M. Gijs and G. E. W. Bauer, Adv. Phys. **46**, 285 (1997).

[16] M. A. M. Gijs, S. K. J. Lenczowski, and J. B. Giesbers, Phys. Rev. Lett. **70**, 3343 (1993).

[17] M. A. M. Gijs, J. B. Giesbers, M. T. Johnson, J. B. F. aan de Stegge, H. H. J. M. Janssen, S. K. J. Lenczowski, R. J. M. van de Veerdonk, and W. J. M. de Jonge, J. Appl. Phys. **75**, 6709 (1994).

[18] J. W. P. Pratt, S.-F. Lee, J. M. Slaughter, R. Loloee, P. A. Schroeder, and J. Bass, Phys. Rev. Lett. **66**, 3060 (1990).

[19] P. Weinberger, P. M. Levy, J. Banhart, L. Szunyogh, and B. Újfalussy, J. Phys: Cond. Matter **8**, 7677 (1996).

[20] R. Kubo, J. Phys. Soc. Jpn. **12**, 570 (1957).

[21] H. E. Camblong, S. Zhang, and P. M. Levy, Phys. Rev. B **47**, 4735 (1993).

[22] M. C. Cyrille, S. Kim, M. E. Gomez, J. Santamaria, K. M. Krishnan, and I. K. Schuller, Phys. Rev. B **62**, 3361 (2000).

[23] D. H. Mosca, F. Petroff, A. Fert, P. A. Schroeder, W. P. Pratt, and Laloee, J. Magn. Magn. Mater. **94**, L1 (1991).

[24] S. Zhang and P. M. Levy, J. Appl. Phys. **69**, 4786 (1991).

[25] G. E. W. Bauer, Phys. Rev. Lett. **69**, 1676 (1992).

[26] D. A. Greenwood, Proc. Phys. Soc. **71**, 585 (1958).

[27] G. D. Mahan, *Many-particle Physics*, *Physics of Solids and Liquids*, 2nd ed. (Plenum, New York, 1990).

[28] H. E. Camblong, P. M. Levy, and S. Zhang, Phys. Rev. B **51**, 16052 (1995).

[29] H. C. Herper, P. Weinberger, A. Vernes, L. Szunyogh, and C. Sommers, Phys. Rev. B **64**, 184442 (2001).

[30] P. Weinberger and L. Szunyogh, Comp. Mater. Sci. **17**, 414 (2000).

[31] L. Szunyogh, B. Újfalussy, and P. Weinberger, Phys. Rev. B **51**, 9552 (1995).

[32] H. C. Herper, P. Weinberger, L. Szunyogh, and C. Sommers, Phys. Rev. B **66**, 064426 (2002).

[33] H. C. Herper, P. Entel, L. Szunyogh, and P. Weinberger, *Ab initio* study of CPP Transport in Fe/Cr/Fe trilayers: influence of transition metal impurities, to be published in MRS Proceedings Vol. 746 (2003).

[34] G. J. Strijkers, J. T. Kohlhepp, H. J. M. Swagten, and W. J. M. de Jonge, Phys. Rev. B **60**, 9583 (1999).

[35] J. J. de Vries, J. Kohlhepp, F. J. A. de Broeder, R. Coehoorn, R. Jungblut, A. Reinders, and W. J. M. de Jonge, Phys. Rev. Lett. **78**, 3023 (1997).

[36] K. Inomata, K. Yusu, and Y. Saito, Phys. Rev. Lett. **74**, 1863 (1995).

[37] R. J. Highmore, K. Yusu, S. N. Okuno, Y. Saito, and K. Inomata, J. Magn. Magn. Mater. **151**, 95 (1995).